Journal of Alloys and Compounds 504S (2010) S123–S128

Contents lists available at ScienceDirect

Journal of Alloys and Compounds

journal homepage: www.elsevier.com/locate/jallcom

Thermal stability and magnetic properties of FeCoBSiNb bulk metallic glasses

Mihai Stoica[a,*], Ran Li[a], Alain Reza Yavari[b], Gavin Vaughan[c], Jürgen Eckert[a,1], Nele Van Steenberge[d], Daniel Ruiz Romera[d]

[a] IFW Dresden, Institute for Complex Materials, Helmholtzstr. 20, D-01069 Dresden, Germany
[b] SIMAP, INP Grenoble, BP 75, Saint Martin d'Hères Campus F-38402, France
[c] European Synchrotron Radiation Facilities ESRF, F-38042 Grenoble, France
[d] OCAS N.V., Pres. J.F. Kennedylaan 3, BE-9060 Zelzate, Belgium

ARTICLE INFO

Article history:
Received 31 July 2009
Received in revised form 31 March 2010
Accepted 2 April 2010
Available online 10 April 2010

Keywords:
Amorphous materials
X-ray diffraction
Synchrotron radiation

ABSTRACT

For the present study, $[(Fe_{0.5}Co_{0.5})_{0.75}B_{0.20}Si_{0.05}]_{96}Nb_4$ bulk metallic glasses (BMGs) were cast as cylinders with 2 mm diameter and 50 mm length. The first crystallized product, the metastable $Fe_{23}B_6$-type like phase, forms as a result of primary crystallization. The thermal stability and the crystallization kinetics were studied using the isochronal and isothermal DSC curves, measured at different heating rate and temperatures. Despite their good glass-forming ability (GFA) and high stability against crystallizations, their incubation time prior crystallization is almost zero. In order to rule-out the complete crystallization mechanism, in situ time resolved studies using the synchrotron radiation were done. The magnetic properties of the BMGs are strongly related to their structure and will be presented as well.

1. Introduction

Since Fe–C–P amorphous alloys were produced in 1965 [1], ferromagnetic metallic glasses and the corresponding nanocrystalline alloys such as FINEMET and NANOPERM [2–4], produced through crystallization from the corresponding amorphous precursors, were intensively investigated because of their excellent soft magnetic properties including relatively high saturation magnetization (M_s) and permeability (μ) as well as low coercive force (H_c) and core loss (W) [5]. Up to now, ferromagnetic amorphous alloys have shown great industrial value for commercial application. Many products consisting of these kinds of metallic glasses have been widely used, for example anti-theft labels and high efficient magnetic transformers in electronic industry. Multicomponent ferromagnetic alloys, such as Fe–(Al,Ga)–(P,C,B,Si), Fe–(Zr,Hf,Nb,Ta)–B and Fe–(Cr,Mo)–(C,B,P) systems [6–13], allow to decrease the critical cooling rate of glass formation, and enable the formation of bulk metallic glasses (BMGs), which not only ensure the fabrication stability during glass formation, subsequent heat treatment processes and shaping operations, but also give ferromagnetic metallic glasses potential applications as advanced structural materials because of their high fracture strength (σ_f) and high corrosion resistance [14].

Recently, (Fe–Co)–B–Si–Nb BMGs were produced which exhibit high glass-forming ability (GFA) as well as good mechanical and magnetic properties (σ_f: ~4000 MPa; M_s: ~1 T; μ: ~12,000; H_c: ~2 A/m) [15,16]. These alloys are regarded as one of the most attractive candidates for application combining the advantages of functional and structural materials. Thus, enormous efforts have been undertaken for this alloy system, especially for the $[(Fe_{0.5}Co_{0.5})_{0.75}Si_{0.05}B_{0.25}]_{96}Nb_4$ glassy alloy, in order to elucidate GFA, thermal stability, mechanical and soft magnetic properties, as well as the effect of minor Cu addition on the physical properties [17–21]. Studies of crystallization and its effect on the magnetic properties in this system are essential for possible commercial application, similar like in case of FINEMET. However, few works have been devoted to this topic so far [20–22]. It is believed that some small additions of Cu may promote the nanocrystallization [23] due to its positive heat of mixing with Fe, Co and Nb [24]. Subsequently, the magnetic properties, as well as the mechanical properties, may become better. However, before changing the composition, it is necessary to study in very detail the behavior of the starting composition, especially the thermal stability and the crystallization way, in order to choose the best procedure to follow. In this paper, $[(Fe_{0.5}Co_{0.5})_{0.75}Si_{0.05}B_{0.25}]_{96}Nb_4$ glassy alloys were chosen for investigation. The GFA and the thermal stability of these alloys were evaluated. The phase evolution, the kinetics parameter and the magnetic properties, including M_s, H_c and T_c were investigated. These results can give more details to understand the relationship between the decomposition of the metastable glassy phase and the magnetic properties and they will be discussed in comparison with other published data.

* Corresponding author. Tel.: +49 351 4659644; fax: +49 351 4659452.
E-mail address: m.stoica@ifw-dresden.de (M. Stoica).
[1] Also at TU Dresden, Institute of Materials Science, D-01062 Dresden, Germany.

0925-8388/$ – see front matter © 2010 Elsevier B.V. All rights reserved.
doi:10.1016/j.jallcom.2010.04.013

2. Experimental procedure

The master alloy was prepared in several steps. First of all, eutectic 25Fe75Nb (wt.%) prealloy was produced by arc melting pure Fe (99.9 mass%) and Nb (99.9 mass%) lumps. The FeNb prealloy, together with the rest of necessary Fe, Co lumps (99.9 mass%), crystalline B (99 mass%) and crystalline Si (99.99 mass%) were melted together by induction heating under protective Ar atmosphere. For this procedure, induction was preferred in order to assure a good homogeneity of the entire master alloy. Pieces of the master alloys were remelted in quartz tubes and then the melt was injected into a water-cooled copper mold in a high-purity argon atmosphere to produce rod-shaped specimens with diameters of 2 and 3 mm, respectively. The thermal stability and the melting behavior of glassy samples were evaluated with a NETZSCH DSC 404 C differential scanning calorimeter (DSC) with a vacuum-tight construction at heating and cooling rates of 20 K/min under a flow of high-purity argon. The activation energy of crystallization for the 2 mm glassy rods was evaluated using a PerkinElmer DSC-7 at a set of heating rates ranging from 5 to 40 K/min adopting the Kissinger method [25]. The crystallization kinetics was studied by means of Jhonson–Mehl–Avrami (JMA) approach [26], using the isotherms measured at different temperatures within the supercooled liquid region (SLR) using the same PerkinElmer DSC-7 device. The structure of the as-cast rods, as well as the in situ crystallization behavior was examined by X-ray diffraction in transmission configuration, using a high energy high intensity monochromatic synchrotron beam ($\lambda = 0.017615$ nm) at ID11 of ESRF Grenoble. The heating in the beam was possible with the samples closed under vacuum in a capillary tube and placed in a LINKAM hot stage device. The heating was performed from room temperature up to 1100 K, at a constant heating rate of 20 K/s. For magnetic measurements, *M–H* hysteresis loops were measured with a vibrating sample magnetometer (VSM) at ambient temperature. The Curie temperature (T_c) for glassy samples was determined using an in-house developed Faraday magnetometer. In order to minimize the errors, the measured data were analyzing using the method proposed by Herzer [27]. The coercivity was measured using a Foerster Coercimat under an applied field high enough to saturate the samples. All magnetic properties were measured under DC magnetic field.

3. Results

It is commonly accepted that the maximum thickness of a BMG is strongly related to the GFA of the respective alloy. In literature it is mentioned for $[(Fe_{0.5}Co_{0.5})_{0.75}Si_{0.05}B_{0.25}]_{96}Nb_4$ glassy alloy a maximum achievable diameter upon copper mold injection casting of 5 mm, for a rod length of 50 mm [17]. If the alloy is fluxed with B_2O_3 prior casting, by water cooling method even 7.7 mm diameter can be achievable, but the rod has only 10–11 mm length [28]. In our work, following the experimental route described in the previous paragraph, we were able to achieve a maximum 3 mm diameter and 70 mm length for which the sample were still fully amorphous. In order to have good statistics and to consider the casting experiments reproducible, for further experiments we used rods with 2 mm diameter and with a length of 70 mm.

3.1. Thermal stability and crystallization kinetics

The DSC trace measured at 20 K/min for bulk glassy 2 mm diameter samples (Fig. 1) shows clearly the glass transition event, followed by the supercooled liquid region (SLR) and crystallization. Additionally, small exothermic events can be observed around 1000 and 1150 K. Further, the alloy melts completely, the melting behavior indicating that the alloy it is not eutectic. The glass transition temperature T_g, the crystallization temperature T_x and the melting temperature T_{liq} were considered to be the offsets of the respective events upon heating. The values, as measured for a heating rate of 20 K/min, are: $T_g = 827$ K, $T_x = 860$, $T_{liq} = 1470$ K. Additionally, in Fig. 1 are marked 3 other temperatures, 902, 985 and 1056 K, respectively. They correspond to the end of the first crystallization, the second exothermic event and the maximum achievable temperature upon heating in the synchrotron beam, respectively. The behavior of the samples at these temperatures will be in detail discussed later, using the X-ray diffraction data. It is interesting to point out that the extension of the SLR is only 33 K and that the first crystallization peak is very sharp.

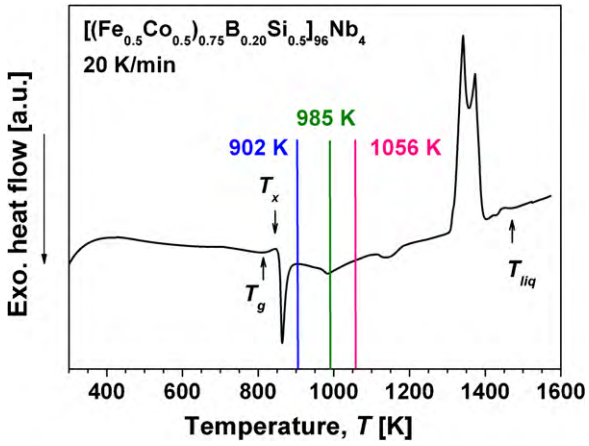

Fig. 1. The DSC traces measured at 20 K/min for $[(Fe_{0.5}Co_{0.5})_{0.75}Si_{0.05}B_{0.25}]_{96}Nb_4$ glassy alloy. The marked temperatures are indications for diffraction data.

Fig. 2 shows the plot of $-\ln(\varphi/T_p^2)$ as a function of the inverse temperature $1000/T_p$. Here T_p represents the peak temperature of the first crystallization event measured in the DSC at different φ heating rates. As can be observed, the data can be fitted with a linear function, the slope of the fitting being proportional with the activation energy necessary for crystallization. From the experimental data, this energy is $E_c = 536$ kJ/mol. The activation energy is quite high, more than double than the energies measured for the well known good glass formers in Zr-based alloy system [29], and relatively close to those measured for other Fe-based glasses [22]. The activation energy is proportional to the energy barrier which the alloy must overpass to jump from a metastable into a stable level. A high value of activation energy indicates a very good stability against crystallization, which is the case of the present studied glassy samples.

In order to study the crystallization kinetics by means of JMA theory, several isothermal annealing were done in DSC. The heating was performed at 20 K/min from room temperature up to temperatures in the SLR. Fig. 3 shows the isothermal DSC traces for samples kept 30 min at $T_x - 12$, $T_x - 15$, $T_x - 17$, $T_x - 20$, $T_x - 23$, where $T_x = 860$ K as measured for a heating rate of 20 K/min. One can observe that the crystallization starts almost immediately, the incubation time is very short. What is different is the time upon the complete crystallization is finished. This time become shorter

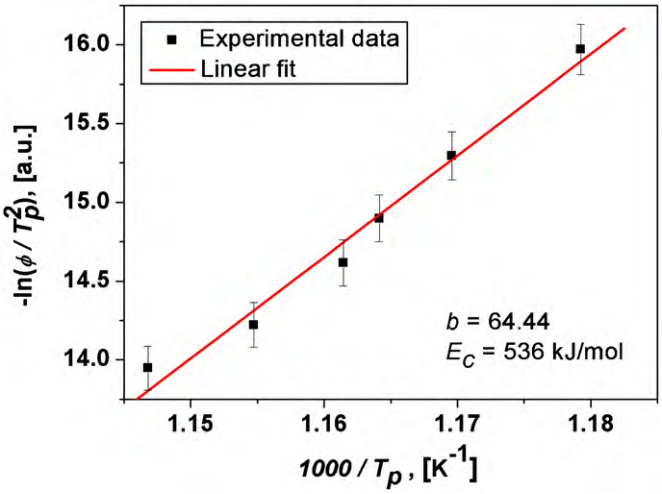

Fig. 2. Evaluation of the activation energy (E_c) by Kissinger plots from the peak temperature of primary crystallization (T_p) for $[(Fe_{0.5}Co_{0.5})_{0.75}Si_{0.05}B_{0.25}]_{96}Nb_4$ glassy alloy.

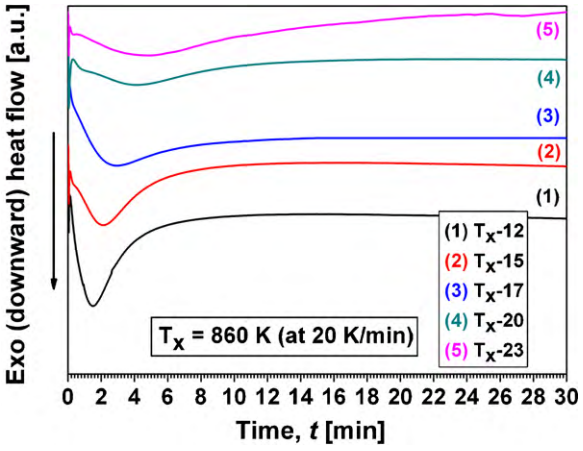

Fig. 3. The DSC traces corresponding to isothermal annealing at different temperatures.

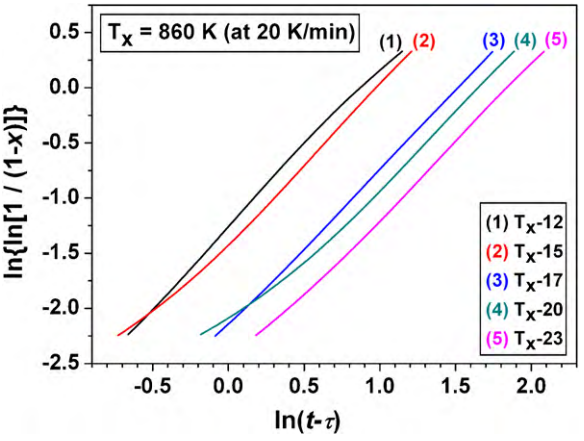

Fig. 4. JMA plots for $10 < x < 75$ (%) crystallized fraction at different temperatures.

when the treatment temperature approaches the T_x. Following the JMA approach, Fig. 4 shows the $\ln\{\ln[1/(1-x)]\}$ as a function of $\ln(t-\tau)$. x denotes the crystallized fraction and its variation in time is proportional with the area closed by the exothermic crystallization event (Fig. 3). The evolution of the crystallized fraction x follows in time a sigmoidal-type curve, which in our case has an almost linear part for values between 0.1 and 0.75 (i.e. corresponds to 10% and 75% volume crystallized fraction). This is why τ, the incubation time, was measured as the point where the crystallized fraction reached 10%. With these data, the Avrami exponent n and the reaction constant k was calculated. The results are summarized in Table 1. The incubation time decreases very fast when the isothermal annealing temperature approaches T_x. In fact, for temperatures above the half of the SLR (ΔT_x is only 33 K in our case, see Table 2), the incubation time τ is less than 40 s, which makes almost impossible its very accurate calculation.

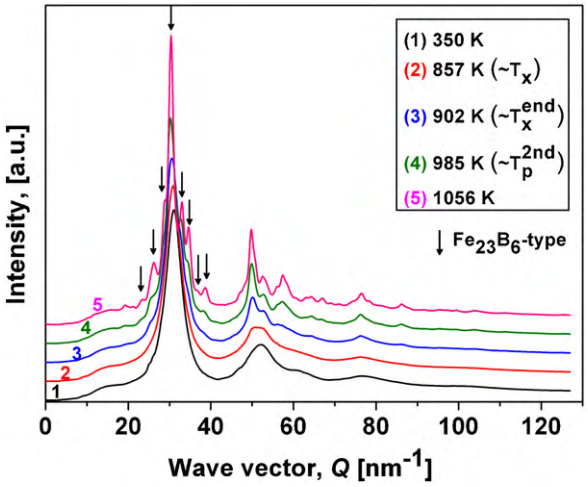

Fig. 5. X-ray diffraction patters showing the structural evolution of $[(Fe_{0.5}Co_{0.5})_{0.75}Si_{0.05}B_{0.25}]_{96}Nb_4$ glassy sample. The temperatures at which the patterns were recorded are marked also in Fig. 1.

Taking into account that the reaction constant k follows a relation of the type $k = k_0 \exp(-E_c/RT)$, where R is the gas constant and T is the temperature, the activation energy for crystallization E_c can be calculated. Its value is 556 kJ/mol, slightly higher than that found by using the Kissinger approach. However, both values are within the measurements errors.

3.2. Time resolved crystallization behavior

Fig. 5 shows several diffraction patterns recorded with the glassy sample at different temperatures: The temperatures are marked in the picture and also in Fig. 1 (the DSC trace for as-cast sample). The structural changes can be easily observed and correlated with the thermal behavior. At room temperature (350 K) the sample is fully amorphous. Once the SLR approaches, the crystallization in the sample starts, but it needs relatively long time for fully crystallization. This is why on the pattern recorded at 857 K (i.e. at T_x) the scatter of the X-ray with the amorphous matrix is still domi-

Table 1
The incubation time τ, Avrami exponent n and reaction constant k calculated using the data measured upon isothermal annealing in the DSC.

Kinetic parameters	Plateau temperature (K)				
	$T_x - 12 = 848$	$T_x - 15 = 845$	$T_x - 17 = 843$	$T_x - 20 = 840$	$T_x - 23 = 837$
Incubation time, τ (min)	0.4	0.65	0.5	1.25	1.7
Avrami exponent, n	1.37	1.48	1.44	1.44	1.43
Reaction constant, k	2.41	2.64	4.54	5.18	6.33

Table 2
Comparison between literature data [17] and our data regarding the as-cast and annealed $[(Fe_{0.5}Co_{0.5})_{0.75}Si_{0.05}B_{0.25}]_{96}Nb_4$ glassy alloy. T_g is the glass transition temperature, ΔT_x the extension of the supercooled liquid region, measured as the difference between crystallization and glass transition temperatures, T_{rg} the reduced glass transition temperature, measured as the ratio between the glass transition and liquidus temperatures, H_c the coercive field, T_c the Curie temperature and J_s the magnetic polarization at saturation.

$[(Fe_{0.5}Co_{0.5})_{0.75}Si_{0.05}B_{0.25}]_{96}Nb_4$	Diameter φ [mm]	T_g [K]	ΔT_x [K]	T_{rg}	H_c [A/m]	T_c [K]	J_s [T]
Literature data	5	820	50	0.587	1.5	692	0.84
Glassy sample	2	827	33	0.56	2.7	720	1.09
Annealed sample	2	–	–	–	43	750	1.21

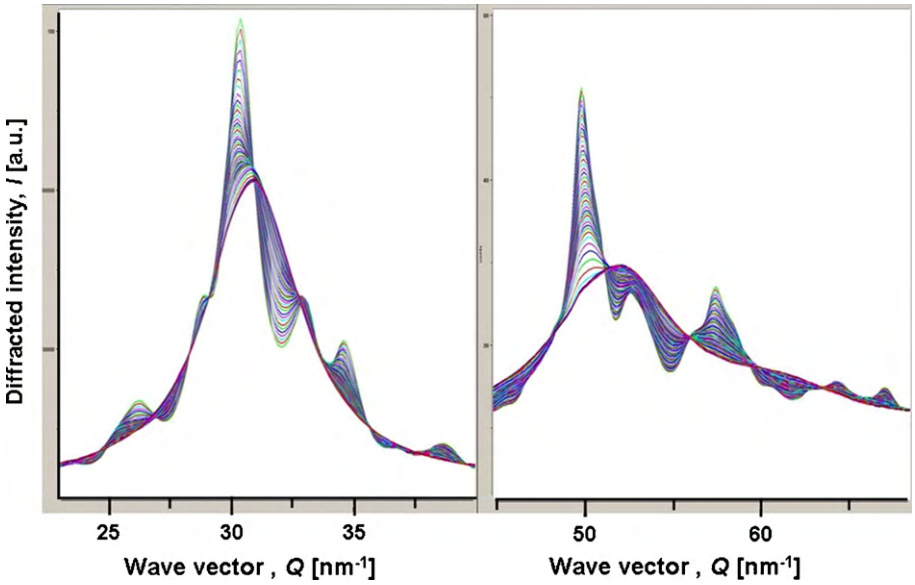

Fig. 6. Time resolved X-ray diffraction patterns by using synchrotron radiation. Details for the first and second halo.

nant. Further, at 902 K, when the primary crystallization finishes, one can see on the pattern some peaks corresponding to a crystalline structure. The first broad peak is still present, which may indicate that still some amorphous matrix is not yet transformed or the crystallized products are in the nm range. In fact, as indicated in the figure, the crystalline peaks can be attributed to an fcc complex structure, the $Fe_{23}B_6$-type phase. These crystalline peaks remain dominant even up to 1056 K, the last achieved temperature for the synchrotron measurements. Comparing with the DSC trace, one can see that at 985 K, the middle of the second crystallization event, some small additional peaks can be seen, (which are not marked in figure) and they could be identified as o-$(Fe,Co)_3B$ or t-$(Fe,Co)_2B$ (the peaks are too weak for a good identification). Most probably, the crystallization sequence is as follow: amorphous → $Fe_{23}B_6$-type plus residual amorphous → $Fe_{23}B_6$-type plus Fe_2B or Fe_3B plus residual amorphous → $Fe_{23}B_6$ plus Fe_2B or Fe_3B. A complete image of the evolution with temperature (from 350 K up to 1056 K) of the first and second amorphous halo is given in Fig. 6. From there one can clearly see that the amorphous matrix gradually transforms in one single crystalline phase.

3.3. Magnetic properties

In order to predict the effect of small addition of other elements as Cu to the mother alloy, the magnetic properties for as-cast and partially crystallized samples were investigated. The partially crystallized sample was obtained by annealing for 10 min at 923 K, i.e. a temperature slightly above the first crystallization event. Fig. 7 shows the DC hysteresis behavior for as-cast and annealed samples. There it is possible to observe that upon annealing the sample remains soft from magnetic point of view, with an increased saturation magnetization. The coercivity of the sample increases as well upon annealing, from 2.7 to 43 A/m, but still it is very low. As observed from DSC and XRD results, the structure of the annealed sample should consist in a mixture of $Fe_{23}B_6$-type phase and a residual amorphous matrix. The variation of the saturation magnetization with temperature is presented in Fig. 8(a), for both as-cast and annealed sample. Due to the technical limitation, the maximum achievable temperature was relatively small, but high enough to enter in the SLR. For the as-cast sample, the Curie temperature measured upon heating is due only by the contribution of the amorphous matrix. Upon cooling, when the sample is partially crystallized, there might be two Curie temperatures, given by the residual amorphous matrix and the contribution of the corresponding crystallized fraction of $Fe_{23}B_6$-type phase. However, even so, only one Curie temperature can be detected, most probably due by the residual amorphous matrix, because the ferromagnetic-paramagnetic transition of the $Fe_{23}B_6$-type phase takes place at a higher temperature than the one attained during the actual measurements. For the annealed (crystallized) samples, there it is only one Curie temperature. Here it should be pointed out that the plots were transformed using the algorithm proposed by Herzer, when the temperatures approach to the Curie temperature [27]. In order to minimize the errors, the experimental results were plotted as $(M_S)^{1/\beta}$ versus T (see Fig. 8(b)), where the exponent $\beta = 0.36$ (the Heisenberg exponent) [27]. The Curie temperature was considered the temperature were the $(M_S)^{1/\beta}$ deviated from linearity.

4. Discussions

Table 2 summarizes the data collected in our work, comparing with what is known from literature [17]. First of all, the reported maximum achievable diameter is 5 mm. In the present work rods with 2 mm diameter were used for measurements. The glass transition temperature of 827 K, higher than the reported one (820 K)

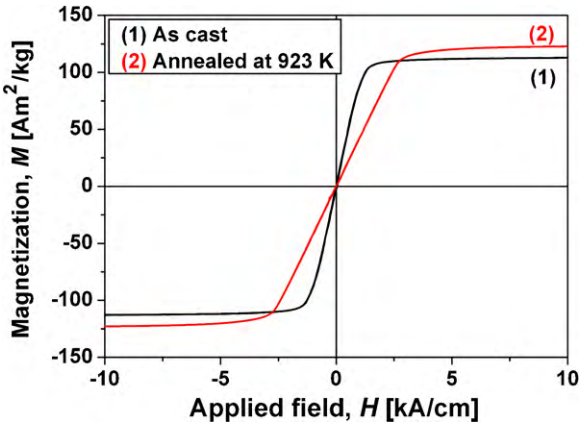

Fig. 7. Hysteresis loops for as-cast and annealed $[(Fe_{0.5}Co_{0.5})_{0.75}Si_{0.05}B_{0.25}]_{96}Nb_4$ 2 mm diameter rods.

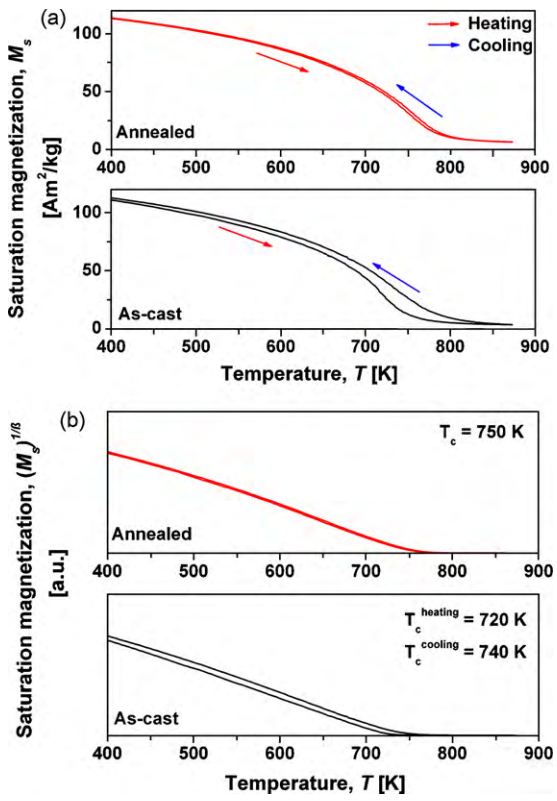

Fig. 8. Thermomagnetic curves for as-cast and annealed $[(Fe_{0.5}Co_{0.5})_{0.75}Si_{0.05}B_{0.25}]_{96}Nb_4$ 2 mm diameter rods: (a) as-measured data, (b) transformed data using the Herzer approach [27].

could indicate a better thermal stability. The extension of the SLR, ΔT_x, was only 33 K in present case, despite the 50 K reported. Smaller is also the reduced glass transition temperature $T_{rg} = T_g/T_{liq}$: 0.56 compared to 0.58. If one considers the extension of the SLR and the reduced glass transition temperature as a gauge for GFA [29], the present investigated alloy seems to have a lower GFA. However, the magnetic properties of the as-cast glassy samples seem to be better: low coercivity, a 30 K higher Curie temperature and also a higher saturation magnetization. In our case, the saturation polarization J_s in T units was calculated using $J_s = 4\pi 10^{-7}\rho M_s$, where M_s is the saturation magnetization in Am^2/kg and ρ is the density. The densities of the samples were measured using the Archimedes method. The values obtained after averaging 25 experimental data were 7689 kg/m^3 for as-cast glassy sample and 7872 kg/m^3 for annealed (partially crystallized) sample.

The differences are quite small, but they may arise, for example, from a small deviation from the overall composition. An increased Curie temperature, followed by increasing in saturation magnetization could be given by a slightly higher Fe content. It was previously shown [17] that the best GFA (but not the best magnetic properties) is obtained in the alloy with Fe:Co ratio 50:50. When the Fe content increases, the magnetic properties become better, the glass transition temperature increases, but the GFA deteriorates.

The present studied glassy samples are very resistant against crystallization. They need high temperature and high energy to crystallize, but once the critical level attained, the crystallization proceeds immediately. This explains the high value of activation energy as well as the very small values found for incubation time (see Table 1). The Avrami exponent, which on average takes the value of 1.43, could indicate some pre-existing nuclei. In literature it is considered that an Avrami exponent of 1.5 = 3/2 is a particular case [30] and it is characteristic for a 3D growth of spherical crystallites, athermal and diffusion controlled (athermal = crystals starts to grow at the same time = crystals of equal size). This is characteristic for primary crystallization way of transformation, in perfectly agreement with our experimental data. The experimental measured values 1.43 of the Avrami exponent, i.e. a bit lower than the particular case of 3/2, may be due by the fact that the pre-existing nuclei are still very small or even not clearly formed. However, it clearly indicates that in this kind of bulk glasses exists a kind of short range order (SRO) which will determine the further crystallization. Most probably, as suggested earlier [31], the atoms are pre-arranged in trigonal prisms, which further will develop in the complex fcc $Fe_{23}B_6$-type structure.

It is commonly accepted that a magnetic BMG shows a very low values of coercivity [32], as it is also our case. If the BMG contains some small volume fraction of crystalline inclusions, the coercivity may seriously increase and this is due to the domain pinning mechanism. If one assumes that there are some nanocrystals or some nuclei, they will not influence the coercivity only if their dimensions are comparable or less that the thicknesses of the domain walls. This very well explains the impossibility to detect such nuclei by X-ray diffraction, even in transmission configuration.

5. Conclusion

$[(Fe_{0.5}Co_{0.5})_{0.75}Si_{0.05}B_{0.25}]_{96}Nb_4$ glassy samples were produced using the injection copper mold casting technique. The samples show soft magnetic properties and a good thermal stability. The amorphous samples may have a kind of pre-defined SRO, clusters or nuclei, ready to crystallize, as indicated by the Avrami exponent $n \sim 1.43$ and the very small incubation time. The energy barrier for crystallization is high, but once the right temperature is attained the crystallization proceeds immediately. The crystallization is diffusion controlled and needs high temperatures to start. Further, transmission electron microscopy studies are required in order to rule-out the exact structure of the sample. The magnetic properties follow the structure. The pre-existing nuclei do not influence the magnetic properties of as-cast samples. Such kind of glassy samples may be good candidates for nanocrystallization studies upon small additions of elements which have positive heat of mixing with the main ingredients Fe and Co (i.e. Cu).

Acknowledgments

The authors thank B. Bartusch, H. Schulze and S. Donath for technical assistance. The work was done under the bilateral collaboration between IFW e.V. and OCAS N.V. One of the authors (R.L.) gratefully acknowledges the financial support from the Alexander von Humboldt foundation. The support from EU and ESRF through the European Network Ductile Metallic Glasses is also fully acknowledged.

References

[1] P. Duwez, S.C.H. Lin, J. Appl. Phys. 38 (1967) 4096–4097.
[2] U. Köster, U. Schünemann, M. Blank Bewersdorff, S. Brauer, M. Sutton, G.B. Stephenson, Mater. Sci. Eng. A 133 (1991) 611–615.
[3] K. Suzuki, A. Makino, A. Inoue, T. Masumoto, J. Appl. Phys. 74 (1993) 3316–3322.
[4] M.E. McHenry, F. Johnson, H. Okumura, T. Ohkubo, V.R.V. Ramanan, D.E. Laughlin, Scripta Mater. 48 (2003) 881–887.
[5] M.E. McHenry, M.A. Willard, D.E. Laughlin, Prog. Mater. Sci. 44 (1999) 291–433.
[6] A. Inoue, Y. Shinohara, J.S. Gook, Mater. Trans., JIM 36 (1995) 1427–1433.
[7] B.L. Shen, A. Inoue, Mater. Trans. 43 (2002) 1235–1239.
[8] N. Mitrovic, S. Roth, J. Eckert, Appl. Phys. Lett. 78 (2001) 2145–2147.
[9] J.Z. Jiang, J.S. Olsen, L. Gerward, S. Abdali, J. Eckert, N. Schlorke-de Boer, L. Schultz, J. Truckenbrodt, P.X. Shi, J. Appl. Phys. 87 (2000) 2664–2666.
[10] A. Inoue, T. Zhang, T. Itoi, A. Takeuchi, Mater. Trans., JIM 38 (1997) 359–362.
[11] A. Inoue, T. Zhang, A. Takeuchi, Appl. Phys. Lett. 71 (1997) 464–466.
[12] S. Roth, H. Grahl, J. Degmova, N. Schlorke-de Boer, M. Stoica, J.M. Borrego, A. Conde, N.M. Mitrovic, J. Eckert, J. Optoelectron. Adv. Mater. 4 (2002) 199–205.
[13] S.J. Pang, T. Zhang, K. Asami, A. Inoue, Acta Mater. 50 (2002) 489–497.
[14] A. Inoue, Acta Mater. 48 (2000) 279–306.

[15] A. Inoue, B.L. Shen, Mater. Trans. 43 (2002) 1230–1234.
[16] A. Inoue, B.L. Shen, C.T. Chang, Acta Mater. 52 (2004) 4093–4099.
[17] B.L. Shen, A. Inoue, C.T. Chang, Appl. Phys. Lett. 85 (2004) 4911–4913.
[18] C.T. Chang, B.L. Shen, A. Inoue, Appl. Phys. Lett. 88 (2006) 011901.
[19] A. Inoue, B.L. Shen, C.T. Chang, Intermetallics 14 (2006) 936–944.
[20] A. Inoue, B.L. Shen, T. Ohsuna, Mater. Trans. 43 (2002) 2337–2341.
[21] R. Li, M. Stoica, J. Eckert, J. Phys.: Conf. Series 144 (2009) 012042.
[22] R. Li, S. Kumar, S. Ram, M. Stoica, S. Roth, J. Eckert, J. Phys. D: Appl. Phys. 42 (2009) 085006.
[23] B.L. Shen, H. Men, A. Inoue, Appl. Phys. Lett. 89 (2006) 101915.
[24] F.R. De Boer, R. Boom, W.C.M. Mattens, A.R. Miedema, A.K. Niessen, Cohesions in metals, North-Holland, Amsterdam, The Netherlands, 1989.
[25] H.E. Kissinger, J. Res. Natl. Bureau Stand. 57 (1956) 217–221.
[26] M. Avrami, J. Chem. Phys. 7 (1939) 1103.
[27] G. Herzer, IEEE Trans. Magn. 25 (1989) 3327–3329.
[28] T. Bitoh, A. Makino, A. Inoue, A.L. Greer, Appl. Phys. Lett. 88 (2006) 182510.
[29] A. Inoue, Acta Mater 48 (2000) 279–306.
[30] B. Wunderlich, Macromolecular Physics, vol.2 Crystal Nucleation, Growth, Annealing, Academic Press Inc., New York, San Francisco, London, 1976.
[31] A. Inoue, B.L. Shen, A. Takeuchi, Mater. Sci. Eng. A 441 (2006) 18.
[32] R. Boll, Weichmagnetische Werkstoffe, VAC GmbH, Ed. Siemens AG Berlin und München, Germany, 1990.